remote sensing

MDPI

Technical Note

The CAESAR Project for the ASI Space Weather Infrastructure

M. Laurenza [1,*], D. Del Moro [2], T. Alberti [1], R. Battiston [3], S. Benella [1], F. Benvenuto [4], F. Berrilli [2], I. Bertello [1], B. Bertucci [5], L. Biasiotti [6], C. Campi [4], V. Carbone [7,8], M. Casolino [9], C. Cecchi Pestellini [10], F. Chiappetta [7], I. Coco [11], S. Colombo [10], G. Consolini [1], R. D'Amicis [1], G. De Gasperis [2], R. De Marco [1], A. Del Corpo [12], P. Diego [1], V. Di Felice [9], L. Di Fino [2], C. Di Geronimo [1], F. Faldi [5], F. Ferrente [13], C. Feruglio [14], E. Fiandrini [5], F. Fiore [14], R. Foldes [15,16], V. Formato [9], G. Francisco [2], F. Giannattasio [11], M. Giardino [17], P. Giobbi [2], L. Giovannelli [2], M. Giusti [1], A. Gorgi [18], B. Heilig [19,20], G. Iafrate [14], S. L. Ivanovski [14], G. Jerse [14], M. B. Korsos [13], F. Lepreti [7,8], D. Locci [10], C. Magnafico [1], V. Mangano [1], M. F. Marcucci [1], M. Martucci [2], S. Massetti [1], G. Micela [10], A. Milillo [1], R. Miteva [21], M. Molinaro [14], R. Mugatwala [2], A. Mura [1], G. Napoletano [15], L. Narici [2], C. Neubüser [22], G. Nisticò [7,8], M. Pauluzzi [5], A. Perfetti [1], S. Perri [7,8], A. Petralia [10], M. Pezzopane [11], M. Piersanti [15], E. Pietropaolo [15], A. Pignalberi [11], C. Plainaki [17], G. Polenta [17], L. Primavera [7,8], G. Romoli [2], M. Rossi [1], L. Santarelli [12], G. Santi Amantini [2], F. Siciliano [11,23], G. Sindoni [17], S. Spadoni [11], R. Sparvoli [2], M. Stumpo [1,2], N. Tomassetti [5], R. Tozzi [11], V. Vagelli [17], N. Vasantharaju [13], A. Vecchio [24,25], M. Vellante [15], S. Vernetto [18], C. Vigorito [18,26], M. J. West [27], G. Zimbardo [7,8], P. Zucca [28], F. Zuccarello [13] and P. Zuccon [3]

1 Institute of Space Astrophysics and Planetology—INAF, Via del Fosso del Cavaliere, 00133 Roma, Italy
2 Department of Physics, University of Rome "Tor Vergata", 00133 Rome, Italy
3 Dipartimento di Fisica, Università degli Studi di Trento, Via Sommarive 14, 38123 Trento, Italy
4 Dipartimento di Matematica, Università degli Studi di Genova, Via Dodecaneso 35, 16146 Genova, Italy
5 Dipartimento di Fisica e Geologia, Università degli Studi di Perugia, Via Pascoli s.n.c., 06123 Perugia, Italy
6 Dipartimento di Fisica, Università degli Studi di Trieste, Piazzale Europa, 1, 34127 Trieste, Italy
7 Dipartimento di Fisica, Università della Calabria, Ponte P. Bucci Cubo 31C, 87036 Rende, Italy
8 National Institute for Astrophysics, Scientific Directorate, Viale del Parco Mellini 84, 00136 Roma, Italy
9 Istituto Nazionale di Fisica Nucleare Sezione di Roma Tor Vergata, Via della Ricerca Scientifica 1, 00133 Roma, Italy
10 Osservatorio Astronomico di Palermo—INAF, Piazza del Parlamento, 1, 90134 Palermo, Italy
12 Istituto Nazionale di Geofisica e Vulcanologia, sede L'Aquila, Viale Crispi 43, 67100 L'Aquila, Italy
13 Department of Physics and Astronomy "Ettore Majorana", Universitá degli Studi di Catania, Via S. Sofia 78, 95123 Catania, Italy
14 Osservatorio Astronomico di Trieste—INAF, Via G.B. Tiepolo 11, 34143 Trieste, Italy
15 Department of Physical and Chemical Sciences, University of L'Aquila, Via Vetoio, 67100 L'Aquila, Italy
16 Laboratoire de Mécanique des Fluides et d'Acoustique CNRS, École Centrale de Lyon, Université Claude Bernard Lyon I, INSA de Lyon, 69134 Écully, France
17 Agenzia Spaziale Italiana, Via del Politecnico s.n.c., 00133 Roma, Italy
18 Osservatorio Astrofisico di Torino—INAF, Via Osservatorio 20, 10025 Pino Torinese, Italy
19 Institute of Earth Physics and Space Science (ELKH EPSS), 9400 Sopron, Hungary
20 Department of Geophysics and Space Sciences, Eötvös University, 1117 Budapest, Hungary
21 Institute of Astronomy with National Astronomical Observatory, Bulgarian Academy of Sciences, 72 Tsarigradsko Chaussee Blvd., 1784 Sofia, Bulgaria
22 Trento Institute for Fundamental Physics and Applications-INFN, Via Sommarive 14, 38123 Trento, Italy
23 Department of Computer, Control and Management Engineering Antonio Ruberti, Sapienza University of Rome, 00185 Rome, Italy
24 Radboud Radio Lab, Department of Astrophysics/IMAPP, Radboud University, P.O. Box 9010, 6500 GL Nijmegen, The Netherlands
25 Laboratoire d'Etudes Spatiales et d'Instrumentation en Astrophysique, Observatoire de Paris, Université PSL, CNRS, Sorbonne Université, Université de Paris, 5 Place Jules Janssen, 92195 Meudon, France
26 Dipartimento di Fisica, Università di Torino, Via Pietro Giuria 1, 10125 Torino, Italy
27 Southwest Research Institute, 1050 Walnut Street, Suite 300, Boulder, CO 80302, USA
28 Institute for Radio Astronomy (ASTRON), Oude Hoogeveensedijk 4, 7991 PD Dwingeloo, The Netherlands
* Correspondence: monica.laurenza@inaf.it

check for updates

Citation: Laurenza, M.; Del Moro, D.; Alberti, T.; Battiston, R.; Benella, S.; Benvenuto, F.; Berrilli, F.; Bertello, I.; Bertucci, B.; Biasiotti, L.; et al. The CAESAR Project for the ASI Space Weather Infrastructure. *Remote Sens.* **2023**, *15*, 346. https://doi.org/10.3390/rs15020346

Academic Editor: Martin G. Mlynczak

Received: 14 November 2022
Revised: 23 December 2022
Accepted: 28 December 2022
Published: 6 January 2023

Abstract: This paper presents the project Comprehensive spAce wEather Studies for the ASPIS prototype Realization (CAESAR), which aims to tackle the relevant aspects of Space Weather (SWE) science and develop a prototype of the scientific data centre for Space Weather of the Italian Space

Agency (ASI) called ASPIS (ASI SPace Weather InfraStructure). To this end, CAESAR involves the majority of the SWE Italian community, bringing together 10 Italian institutions as partners, and a total of 92 researchers. The CAESAR approach encompasses the whole chain of phenomena from the Sun to Earth up to planetary environments in a multidisciplinary, comprehensive, and unprecedented way. Detailed and integrated studies are being performed on a number of well-observed "target SWE events", which exhibit noticeable SWE characteristics from several SWE perspectives. CAESAR investigations synergistically exploit a great variety of different products (datasets, codes, models), both long-standing and novel, that will be made available in the ASPIS prototype: this will consist of a relational database (DB), an interface, and a wiki-like documentation structure. The DB will be accessed through both a Web graphical interface and the ASPIS.py module, i.e., a library of functions in Python, which will be available for download and installation. The ASPIS prototype will unify multiple SWE resources through a flexible and adaptable architecture, and will integrate currently available international SWE assets to foster scientific studies and advance forecasting capabilities.

Keywords: space weather; solar photosphere; solar chromosphere; solar corona; solar activity; solar wind; solar energetic particles; earth's magnetosphere; earth's ionosphere; earth's plasmasphere; planetary space weather; galactic cosmic rays

1. Introduction

The understanding of basic processes of plasma physics from the Sun to Earth is a unanimously recognised primary interest both for making significant scientific advances in space weather (SWE) research as well as enhancing our capabilities to predict SWE effects and ensure effective mitigation (e.g., [1]). Recently, the concept of SWE was extended to planetary environments and is referred to as planetary space weather (PSW, [2,3]), in which the solar activity variability and/or interplanetary space dynamics determine the variability in planetary environments.

Despite many decades of extensive research across solar, interplanetary, magnetospheric/ionospheric, and planetary physics, the study of the chain of SWE-associated phenomena, as well as the assessment of impacts and forecasting of SWE events, demands a further continuing effort. In particular, there is a need for more comprehensive studies that include multiple aspects of SWE when addressing the problem of the origin and evolution of solar eruptive events, as well as the impact on Earth's magnetosphere/ionosphere and other planetary systems. Moreover, SWE spans a number of well-established communities, but they have evolved independently over decades, utilising significantly different data content, storage, and handling.

Efforts to support and foster scientific studies through dedicated databases (DBs), and collections of disparate resources, including models and tools, are being pursued by many institutions and organisations, including the National Aeronautics and Space Administration (NASA), the European Space Agency (ESA), and many national agencies.

The USA National SWE Program Strategic Plan (started in 1995, reviewed and redefined in March 2019) has the primary goal of discovering and understanding the physical conditions and processes that produce SWE and its effects. Similarly, the NASA program "Living With a Star" (LWS (https://lws.gsfc.nasa.gov, accessed on 1 September 2021)) focuses on the science needed to comprehend the aspects of the Sun and space environment that most directly influence life and society. In addition, LWS supports scientific research and technology investigations in key areas, spanning different scientific disciplines, as well as the development of comprehensive models with forecasting capabilities. Such strategic models are made available (e.g., via the Community Coordinated Modeling Center (CCMC) (https://ccmc.gsfc.nasa.gov, accessed on 1 September 2021)) to be used by the scientific community and to be potentially translated into operations. The National Oceanic and Atmospheric Administration's (NOAA) Space Weather Prediction Center (SWPC (https://www.swpc.noaa.gov, accessed on 1 September 2021)) is more operation-

oriented, providing the official space weather alerts and warnings for the United States and multiple space weather monitoring datasets, as well as numerous products (tools, graphics, and subsidiary datasets) to help research scientists in both understanding and making use of the vast array of SWE information, as well as in forecasting the upcoming space activity and in modelling longer-term outlooks for future events.

The ESA Space Situational Awareness (SSA) programme started in 2009 and ended in 2019; in particular, the SSA SWE segment aimed at monitoring and predicting the state of the Sun and the interplanetary and planetary environments, including Earth, which can affect infrastructures, thereby endangering human health and safety. From 2020, the ESA's Space Safety programme has built on the work carried out by SSA. In this context, the SWE Service Network is currently focusing on the development of both key models and user-tailored services, as well as other building blocks to provide end users with reliable and timely SWE information. The online component of the SWE Services can be accessed via the SWE Portal (https://swe.ssa.esa.int, accessed on 1 September 2021). Furthermore, the strategic orientations of the Horizon 2020 Program for the last few years have specifically supported the production of SWE models and tools to improve forecasting capabilities, with an emphasis on the connection between SWE physical processes occurring sequentially or simultaneously in different domains.

During FP7 and H2020 Framework Programs, the European Commission financed several projects with the aim of enhancing the efficiency of data access for heliophysics studies. Among those, it is worth citing HELIO [4,5], CASSIS [6], SOTERIA [7], HELCATS [8], and HESPERIA [9]. These projects involved several partners from all over the world and explored the many aspects of building open tools for data access and exploitation and making those tools available to the extended SWE community.

In the Italian context, the Italian Space Agency (ASI) has produced a SWE roadmap [10] for a long-term strategy to support the future scientific research of SWE and the realisation of a national scientific data centre for space weather, termed ASI SPace Weather InfraStructure (ASPIS), while strengthening synergies among the SWE/PSW Italian groups in a strong collaborative environment. Therefore, the Comprehensive spAce wEather Studies for the ASPIS prototype Realization (CAESAR) project was selected to reach such goals. CAESAR is coordinated by the National Institute of Astrophysics (INAF) and is presented in this manuscript.

CAESAR addresses scientific problems pertaining to the origin and evolution of solar eruptive events and their propagation and impacts through an unprecedented, comprehensive, multidisciplinary, and integrated approach. This encompasses the whole chain of phenomena from the Sun to Earth, as well as to other planets. In this endeavour, it is crucial to exploit a variety of products (datasets, codes, models) that will ultimately populate the ASPIS prototype. This is intended to unify multiple SWE resources in a flexible architecture to allow users to perform advanced scientific studies, both through a web interface and a dedicated application called ASPIS.py. A keyword metadata system will enhance search capabilities, especially as data volumes grow with recorded events.

The ASPIS prototype will be open-source, allowing scientists to study problems that span disciplinary boundaries. It will create an environment where researchers can investigate, model, and uncover the linkage between solar phenomena, interplanetary disturbances, and impacts on the planets (especially Earth).

In this article, we outline the basics of the CAESAR project: Section 2 provides an overview, describing the objectives and work breakdown structure used; Section 3 describes the science that CAESAR has been designed to address; Section 4 outlines the ASPIS prototype; and Section 5 describes the methods used to disseminate the results. Conclusions are drawn in Section 6.

2. CAESAR Overview

The scientific targets of CAESAR are multi-faceted, and its main objectives (amongst others) include:

1. To advance our understanding of the origin and evolution of SWE phenomena;
2. To provide both new and long-standing data, codes, and models to populate the ASPIS prototype;
3. To design the architecture and realise the ASPIS prototype with findability, accessibility, interoperability, and reusability data (FAIR-data), and flexible and user-friendly infrastructure;
4. To pave the way for future reliable and advanced SWE forecasting capabilities;
5. To ensure the efficient dissemination of results and infrastructure and foster future SWE studies.

In order to achieve these goals, CAESAR is organised into three nodes (NODE 1000, NODE 2000, NODE 3000), managed and coordinated by the Work Package (WP) 0.1: Management (Figure 1).

NODE 1000 is dedicated to scientific investigations that are performed to attain objectives 1., 2., and 4. in the list above. In particular, it investigates all of the relevant aspects of SWE in different domains (or science cases): the active Sun as the source of SWE drivers (e.g., flares, coronal mass ejections (CMEs), solar energetic particles (SEPs)); interplanetary space, where SWE drivers propagate determining perturbed conditions; solar-wind–Earth's magnetosphere coupling; Earth's magnetosphere–ionosphere coupling; planetary space weather; galactic cosmic ray modulation; and SWE hazards for technological systems and human exploration.

As shown in Figure 2, NODE 1000 includes seven high-level (HL) WPs that reflect the science cases described above. Based on the proposed scientific studies, HL WPs have one contact person, each of different institutions according to the expertise needed to manage and coordinate the investigations related to one application domain (e.g., the active Sun, interplanetary space, and so on) as well as the interaction with other HL WPs. Moreover, each HL WP comprises several individual WPs, in synergy with each other, managed by a WP leader with recognised experience to address the specific tasks of each domain. Nevertheless, a strong collaboration also exist between WPs of different HL WPs and with the other two nodes.

NODE 2000 is dedicated to fulfilling objective 3. listed above. In order to develop the ASPIS prototype, the NODE is organised into three HL WPs for: the database, the interface, and the metadata structure (see Figure 3). Each HL WP is divided into three WPs for specific activities (for instance, ASPIS design, ASPIS implementation, and product management) that have a strong synergy with each other and with those of the other HL WPs.

NODE 3000 is devoted to performing dissemination activities in order to reach goal 5. and is also divided into three WPs (see Figure 4) for: the construction of the CAESAR website; the dissemination to the SWE scientific community, to students of universities and schools, and to the general public; and the organisation of a workshop at the end of the project.

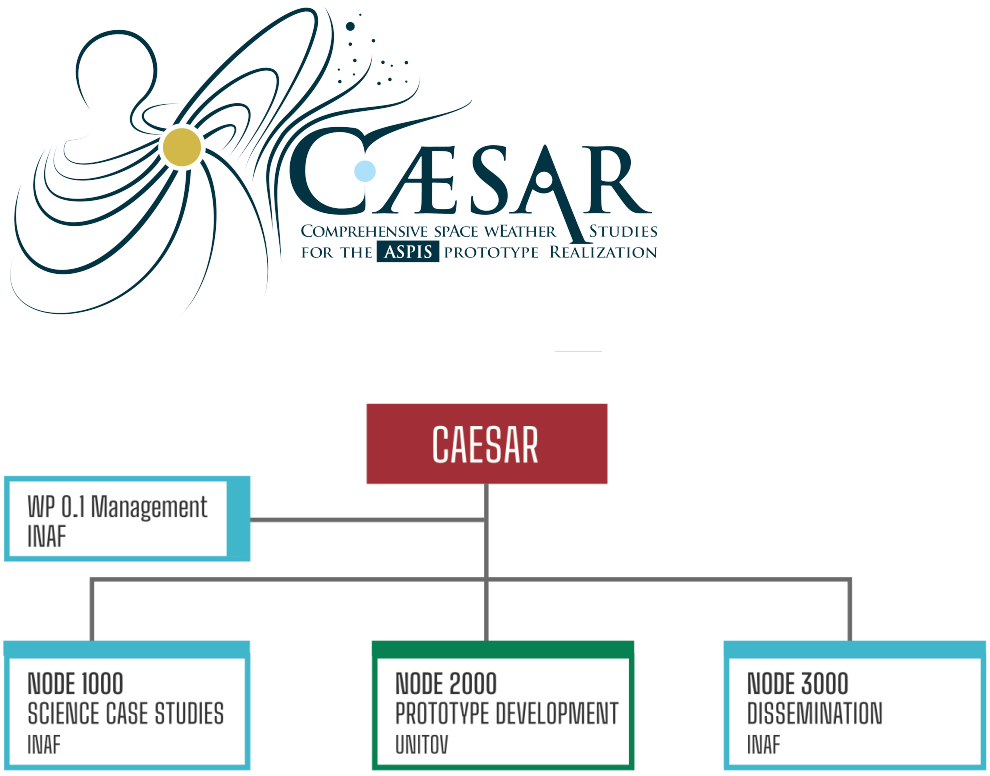

Figure 1. (**Top**) CAESAR logo (courtesy of Carmelo Magnafico). (**Bottom**) Work breakdown structure of CAESAR.

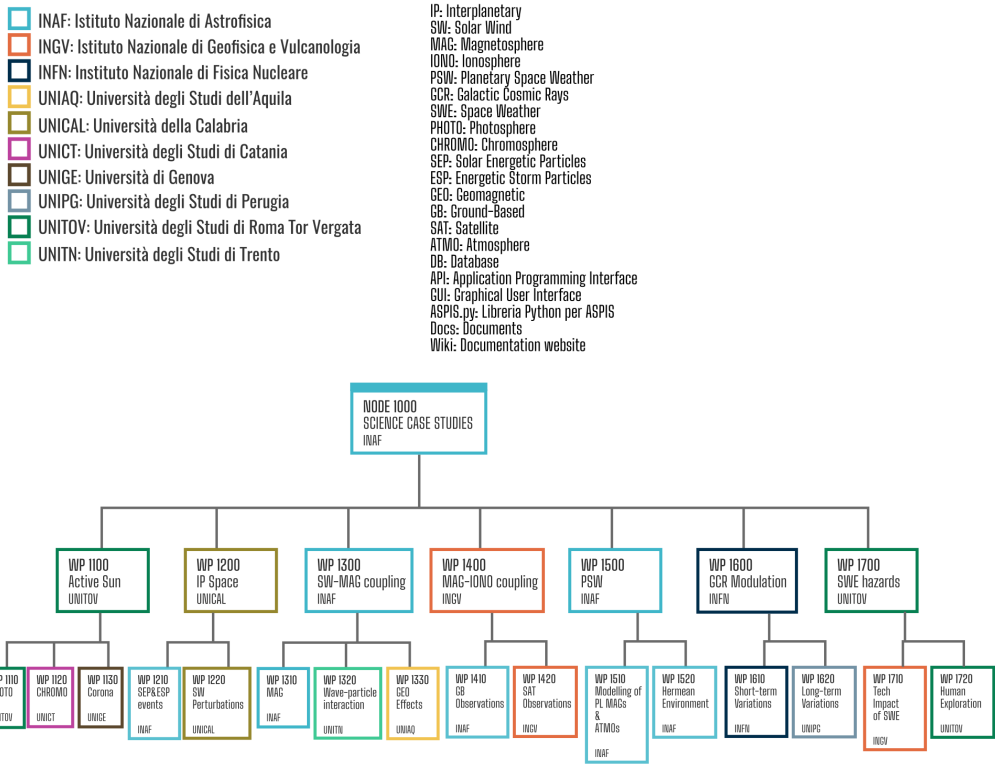

Figure 2. Work breakdown structure of NODE 1000.

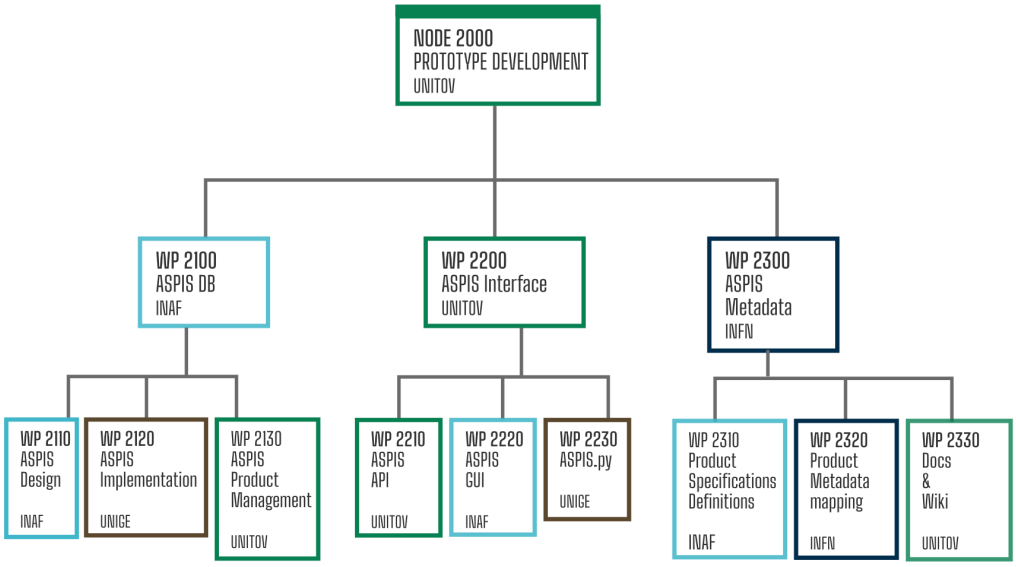

Figure 3. Work breakdown structure of NODE 2000. Colors indicate institutions described in the legend of Figure 2.

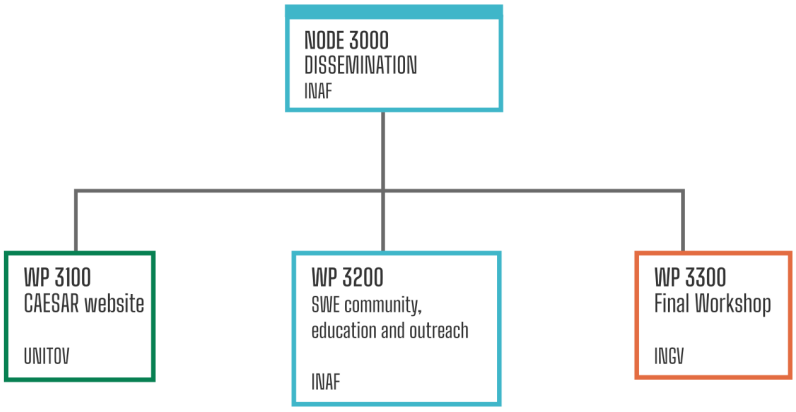

Figure 4. Work breakdown structure of NODE 3000. Colors indicate institutions described in the legend of Figure 2.

3. CAESAR Science

SWE manifests in many forms, from the background solar wind and the interplanetary magnetic field (IMF) frozen in the solar wind plasma to transient short-lived energetic events, such as the sudden release of radiation into space by solar flares, the expulsion of CMEs, EUV waves, and the acceleration of SEPs at CME-driven shocks and flare sites. Ultimately, the Sun is the source of all SWE phenomena; therefore, the first domain of investigation in the SWE chain is naturally devoted to understanding the solar conditions that favour the development of solar eruptions and related energetic phenomena.

The eruptive phenomena originate in the evolution of the magnetic field through the convective zone of the Sun (where the emergence and transport of magnetic fields occur) to the solar atmosphere, i.e., photosphere, chromosphere, and corona [11–17]. These external layers are the sites of explosive solar events connected to the reconfiguration of the magnetic field, observed at the photosphere as magnetic footpoint motions, and the associated energy release responsible for flares, CMEs, and SEPs [18,19]. The interconnectedness of the underlying physical processes (the evolution of magnetic field in active regions, energy build-up and release, triggering instabilities, magnetic reconnection processes, particle acceleration mechanisms) is complex and still not fully understood [20]. Much work has

been carried out within the Italian community regarding flare triggering (e.g., [21,22]), SEP acceleration [23,24], and flare and SEP forecasting [25–27], also with the introduction of new metrics and their evaluation through machine learning (ML) techniques [28,29]. Following such studies, the WP1100 aims to understand the link between features in the layers of the solar atmosphere (e.g., the magnetic field in the photosphere, filaments and prominences in the chromosphere, X-ray and EUV emission in the corona) and the occurrence of the SWE drivers. For instance, photospheric magnetic imprints [30–32] and chromospheric features such as bright faculae and dark filaments, which are indicative of different modes of interaction between the solar plasma and localised magnetic fields, are investigated in WP1110 and WP1120, respectively, for: evaluating the level of magnetic activity, which has an important impact on the variability of the total solar irradiance, and providing some hints on flare occurrence. Moreover, in the chromosphere, we are studying important signatures of flare occurrence, such as filament activation and rising during the pre-flare phase, bright ribbons, kernels, H_α post-flare loops, chromospheric evaporation, and so on. Filament activation and rise, as observed in the chromospheric H_α line, are in fact some of the well-known precursors of solar flares, and being able to detect these signatures can be an important tool for providing an alert of an approaching flare occurrence. Prominences observed on the limb can provide important hints on the structuring of the active region's magnetic field and are used as context information in case of flare occurrence. In addition, WP1130 is developing several computational methods, e.g., for the desaturation of EUV images, by using diffraction effects present in the EUV saturated images to recover the physical and morphological information of the region that emits the largest part of the energy. The desaturated images can then be used to better study the EUV lower coronal dynamic structures [24,33,34] along with the CME kinematics through coronographic images [35].

The propagation of SWE drivers in the interplanetary space [36–38] can create perturbed solar wind conditions strongly affecting the near-Earth/planets systems in different ways [39–41]. Thus, it is mandatory to understand the processes involved in the dynamics and propagation of solar wind perturbations (e.g., the CME structure, evolution of CME magnetic clouds and shocks, solar wind drag, IMF field line meandering, particle diffusion), and how the features of the background solar wind streams can be relevant from an SWE perspective (e.g., turbulence, intermittency, Alfvenicity; [42,43]). In addition, the study of the so-called energetic storm particles (ESPs, [44]) associated with in situ CME-driven shocks represents a powerful way to test particle acceleration/transport theories (such as diffusive shock acceleration, stochastic acceleration, drift/surfing acceleration, anomalous diffusion) against in situ observations [45–51]. So far, our knowledge and understanding of SWE phenomena in the interplanetary space has relied on observations mainly made from Earth's orbit. Currently, a new leap is possible for providing new insights by taking advantage of the potential offered by the most recent space missions from different vantage viewpoints. Indeed, novel and unprecedented high-resolution observations are being recorded close to the Sun by the Parker Solar Probe ([52], 0.2–0.3 AU, launched in August 2018), Solar Orbiter ([53], 0.28–29 AU, launched in February 2020), and BepiColombo ([54], 0.29–0.4 AU, launched in October 2018). The WP1200 will contribute toward shedding light on the mechanisms leading to the acceleration and transport of energetic particles during SEP and ESP events and to perturbed conditions in interplanetary space through the activities of WP1210 and WP1220, respectively. The WP1210 is analysing particle data to obtain properties (e.g., flux profile, spectra) of SEP and ESP events from the aforementioned fleet of spacecraft presently available. Data from the ground-based network of neutron monitors complement the study of SEPs at relativistic energies when a ground-level enhancement (GLE) occurs. This WP is also performing a comparison of the obtained ESP spectra with expectations of acceleration and transport models [49,51]. The role of magnetic turbulence and intermittency nearby interplanetary shocks is also studied within WP1220, in close collaboration with WP1210, to gain further insight into the role played by these processes in particle acceleration and transport at interplanetary shocks. The properties of

magnetic turbulence upstream and downstream of interplanetary shocks associated with ESP events are analysed by calculating power spectral densities (PSDs) of the magnetic field (see e.g., [55,56]). Moreover, in order to obtain information about the intermittency level of turbulent fluctuations, the structure functions (SFs) of the magnetic field component fluctuations are being computed.

Data from currently available spacecraft can also be utilised to assess the Alfvénicity of solar wind streams by analysing the correlation between velocity and magnetic field fluctuations and verifying the condition of near-incompressibility. Indeed, Alvfénic solar wind streams have been shown to be related to high-intensity long-duration continuous AE activity (HILDCAA)-like events (e.g., [43,57]) as monitored by the auroral electrojet (AE) index, but also a long-recovery phase of the SYM-H index [58]. Therefore, this investigation is carried out in synergy with WP1310 (see below) toward the aim of characterising the magnetospheric dynamics related to these events both at high latitudes (auroral indices) and low latitudes (e.g., SYM-H).

WP1220 investigates the evolution and propagation of CMEs in the interplanetary space through a probabilistic drag-based model [59–61] by using the CME features obtained by WP1100. The model evaluates the CME characteristics at arrival at Earth and other planetary environments, which serve as an input to both WP1300 and WP1500. At these locations, the large-scale magnetic configuration of the CME interplanetary counterpart is also obtained through a Grad–Shafranov (GS) reconstruction [62–64]. This last activity is developed in synergy with WP1610, where the results of the GS reconstruction of magnetic clouds are used in the study of sporadic variations in galactic cosmic ray intensities, such as Forbush decreases [64].

At Earth, the solar wind perturbations may cause highly disturbed states in the magnetosphere and ionosphere during the so-called geomagnetic storms and substorms, involving changes in the magnetospheric circulation and plasma energisation and intensification of the magnetospheric and ionospheric current systems [65–71]. The solar wind momentum and mass are transferred most efficiently through the reconnection processes during periods of southward IMF, so that the IMF orientation is a crucial parameter for the geo-effectiveness of CMEs. Nevertheless, also during northward IMF periods, reconnection at the poleward of the cusps [72] or Kelvin–Helmholtz waves at the magnetosphere flanks [73] can occur. As a matter of fact, the solar wind–magnetosphere–ionosphere coupling results in a very complex system composed of largely different plasma populations pervaded by a variety of current systems. The main population in terms of mass density is the plasmasphere, an extension of the ionosphere to the magnetosphere up to 5–6 Earth radii. It is mainly composed of cold plasma ($\sim$1 eV) and its shape is highly influenced by the geomagnetic activity. The plasmasphere partially overlaps with more energetic plasmas, such as the ring current (1–500 keV), which dominate the energy density, and the radiation belts (100 s of keV to MeV), which are mainly responsible for spacecraft damages in the near-Earth region [74]. The cold plasma is central in the plasma-waves excitation and interaction with ring current and radiation belts [75]. Moreover, dramatic ionosphere modifications can be caused by ionising radiation from flares and SEPs. Despite many phenomena being unveiled through in situ measurements made by near-Earth plasma missions in the last few decades, all of the main aspects pertaining to this system that play a crucial role for space weather, namely the energy and plasma transfer from the solar wind, the system internal response—chiefly related to the magnetotail physics—and the system coupling with the ionosphere, are still far from being fully comprehended [76]. For instance, the existence of the storm–substorm interaction remains one of the most controversial questions of magnetosphere dynamics [77]. The combination of in situ and multi-scale ground-based observations together with the development of new data analysis techniques and data-driven models ([78]—see also the CCMC)—is vital for pursuing scientific studies of the magnetosphere structure and dynamics and the ionospheric response. Thus, WP1300 will better understand the geomagnetic response during SWE events, with respect to the magnetosphere structure and dynamics in the larger context of the solar wind–

magnetosphere coupling. To this end, WP1310, WP1320, and WP 1330 are dedicated to phenomena in specific magnetospheric regions, i.e., the outer magnetosphere, the radiation belts, and the plasmasphere, respectively. In particular, WP1310 is dedicated to analyses of ESA-Cluster, NASA-Time History of Events and Macroscale Interactions during Substorms and NASA-Magnetospheric Multiscale plasma and magnetic field data in order to study the occurrence of reconnections at the magnetospheric boundaries by using the Walén test [79,80], as well as to model the magnetosheath parameters, magnetopause compression, and magnetospheric current systems by using a modified version of the Tsyganenko and Sitnov [81] (hereafter TS04) model (assuming input parameters from WP1220 as far as the interplanetary medium is concerned). WP 1330 focuses on the determination of the equatorial plasma mass density distribution using geomagnetic pulsations detected by the European quasi-Meridional Magnetometer Array (EMMA) [82], employing both assisted and automated algorithms [83–85]. Moreover, WP1320 is dedicated to the plasma acceleration from the magnetosphere into the ionosphere, focusing on the wave–particle interaction analysis by combining both magnetospheric and ionospheric satellites and the TS04 magnetospheric model. Indeed, despite the energy carried by waves in the magnetosphere (compressive and/or Alfvén) being much lower than the one stored from particle precipitation in the ionosphere, it is well known that such waves play a key role in the magnetospheric dynamics.

The WP1400 studies the physical state of the ionosphere [86,87] in order to address, for example, the complex and dynamic system of ionospheric currents resulting from the magnetosphere–ionosphere coupling [88–90], which amplifies as a consequence of SWE events. In particular, the activities of WP1410 and WP1420 exploit ground-based and spaceborne data, respectively. In more detail, WP1410 takes advantage of information mainly from ionosonde facilities and coherent high-frequency radar networks. Ionosondes managed by INGV at Rome and Gibilmanna (Italy) and co-managed by INGV at Tucuman and Bahia Blanca (Argentina) provide both the ionospheric vertical electron density and some specific ionospheric parameters [91–93] that are essential for a detailed picture of the ionospheric conditions over the ionosonde locations, which is crucial for radio communications in the high-frequency domain.

Observations from the Super Dual Auroral Radar Network (SuperDARN) are also used. The network consists of over 30 coherent high-frequency radars in both hemispheres at latitudes from middle to polar and is aimed at investigating the convection of ionospheric plasma. This is achieved by analyzing the Doppler phase shift of radio signals backscattered by density irregularities in the E and F ionospheric regions [94]. Since these irregularities follow the motion of the surrounding plasma, it is possible to generate maps of large-scale ionospheric convection, which is strongly dependent on the variation in the conditions of the magnetised interplanetary plasma and magnetosphere [95]. In addition, the estimation of the cross-polar cap potential, namely the maximum potential difference in the polar cap, allows for an assessment of the energy transferred from the magnetosphere to ionosphere [96,97].

In order to better understand the processes underlying magnetosphere–ionosphere coupling, it is also critical to characterise the physical parameters describing the topside ionosphere via in situ measurements. To this aim, WP1420 is devoted to analysing the behavior of physical quantities, such as electron density, temperature, and electrical conductivity, which are excellent proxies of dynamical processes occurring especially at high latitudes, as well as geomagnetic field and ionospheric indices. In situ data from two flagship missions for Earth observation currently in orbit at approximately 500 km altitude are used: the ESA's Swarm constellation [98] and the Limadou/China Seismo-Electric Satellite (CSES) mission [99]. The investigation of small-scale irregularities can be carried out through the calculation of ionospheric indices based on both in situ and remote sensing measurements. In particular, the Rate Of change in electron Density Index (RODI) and the Rate Of change in Total electron content Index (ROTI) are well established proxies of irregularities on a wide range of spatial scales [100–102]. More recently, the Rate Of

change in electron TEmperature Index (ROTEI) has been introduced to capture small-scale variations in electron temperature, which may play a crucial role in the energetic budget of the ionospheric plasma and the occurrence of irregularities [103]. For these reasons, RODI, ROTI, and ROTEI indices will be computed and mapped starting from Swarm observations and data from GPS satellites in view [104]. Finally, an estimation of the geoelectrical field at Swarm altitudes will be provided by using the MA.I.GIC. model [105]. The model is based on the fact that, in the frequency space, the geoelectric and geomagnetic fields are linked by impedance, which ultimately depends on electrical conductivity. Thus, by using geomagnetic field observations acquired by the Swarm mission, it is possible to retrieve the geoelectric field and, by invoking Ohm's law, the current density.

The SWE impact on other planets depends on several factors, such as the presence of an intrinsic dipolar magnetic field (such as Mercury, Jupiter, or Saturn) and/or of an atmosphere (such as Mars or Venus), generally causing effects on planetary magnetospheres and atmospheres by not only enhancing their dynamics but also altering their structure and composition. The investigation of solar wind plasma interaction with different environments in our Solar System is paramount, as the comprehension of a planetary environment other than Earth is a precious way to investigate the many complex and different aspects of Sun–planet interactions [3]. The purpose of WP1500 is to improve our knowledge of the physical processes involved in the coupling between solar wind and planetary magnetospheres during SWE events, as well as the variability of atmospheres/exospheres. In particular, numerical simulations of encounters of solar wind plasma with different magnetosphere and atmosphere environments in our Solar System are the main investigation topic of WP1510. We study coupled Kelvin–Helmholtz (KH) and tearing mode (TM) instabilities as a result of mixing layer dynamics formed when distinct solar-wind–magnetosphere–atmosphere encounters occur. These studies can address magnetic reconnection phenomena that are believed to be one of the key drivers of plasma transport. Earth's and other planetary magnetospheres are excellent laboratories for investigating them. The magnetospheric instability model [106] is utilised for studying observed asymmetries and, generally, the coupling between external and internal layers after the impact of SWE events. In addition, atmospheric studies on how the chemical composition of planetary atmospheres such as Venus and Mars changed over billions of years, owing to both the solar radiation and CME-altered mass loss and the chemical profiles of planetary atmospheres, are performed. The coupling between solar wind and the Mercury environment (WP1520) is the subject of a study that has the following architecture. There is a model that takes the actual solar wind conditions as inputs (obtained from WP1220) and estimates the solar wind precipitation onto the surface of Mercury in these different SW scenarios. The model is an evolution of [107] and is compared with other studies, such as [108], or more recent ones [109]. Extreme cases, such as those in [110], can also be used as inputs. Then, a Monte Carlo model of the exosphere of Mercury can be used [111], which can simulate the effect of plasma precipitation on the exosphere of Mercury. Finally, the results can be compared with actual Na exospheric observations performed with the THEMIS solar telescope [112] (the whole database for years 2009–2013 will be available). In this way, the whole chain can be tested and the mechanism of environmental modifications will be better understood.

SWE events modulate the intensity of galactic cosmic rays (GCRs) in the whole heliosphere. In particular, the large-scale topology of the magnetic field in interplanetary perturbations can produce GCR depressions called Forbush decreases (FDs) at short-term temporal scales (e.g., [64]). Moreover, the GCR intensity and spectra undergo important global changes on longer time scales due to the modulation by solar activity (11-year Schwabe cycle, 22-year Hale cycle). The physical mechanisms governing such processes (convection, diffusion, drifts, adiabatic energy losses) are generically understood, while the changing interplay among the various mechanisms at the different time scales and IP conditions are still under investigation [113]. An improved comprehension of such processes would have important implications for both GCR modulation models and the prediction of the GCR flux in the interplanetary space, which constitute a problem for space

missions and air flights [12,114–119]. The purpose of WP1600 is a deeper understanding of both the physical mechanisms underlying GCR modulation at different spatial and temporal scales and the implications of solar activity on charged particles propagation and our prediction capabilities. The WP1610 and WP1620 are devoted to short-term and long-term GCR intensity variations, respectively. In the framework of WP1610, data from several space missions and ground-based neutron monitors are being analysed in order to study the temporal evolution of GCR fluxes. In particular, work is currently focusing on the analysis of the data from the AMS-02 magnetic spectrometer on board the International Space Station using observations of daily proton fluxes from 1 GV to 100 GV over the period from 20 May 2011 to 29 October 2019 [120] and combining them with available results from other missions, with a particular focus on the PAMELA spectrometer and the Rome and Testa Grigia neutron monitors. Moreover, test-particle simulations on the background magnetic field, which consists of a GS reconstruction performed in WP1220, are being performed to model particle propagation during Forbush decreases and compare it to particle data. The WP1620 exploits the availability of accurate long-term measurements to develop numerical models describing the transport of GCR radiation inside the heliosphere. The different models will be tested, validated, and exploited to calculate GCR differential fluxes in different epochs and locations in the heliosphere.

Finally, SWE events have a substantial impact on spaceborne and ground-based critical infrastructures, the human body, and human activities [121–124]. For instance, SWE events can induce: an onset of sharply increased geoelectric fields and associated geomagnetically induced currents (GICs) leading to the shorting of electrical power grids [125]; the growth of ionospheric irregularities causing a malfunctioning or loss of lock (LoL) of global navigation satellite systems as the global positioning system [126]; an increase in the radiation environment and high-dose rates in the whole heliosphere, which is also critical for space exploration, as human spaceflights are being prepared for lunar and Mars missions. The purpose of WP1700 is the assessment of the SWE impact on Earth's environment down to the ground. Thus, the WP1710 and WP1720 are devoted to the SWE hazards for technological systems and the human body, respectively. In order to be able to mitigate possible damages on critical infrastructures, it is necessary to recognise whether a specific solar event could cause specific GIC-originating variations in the geomagnetic field. Most of the investigations performed so far have focused on associating the growth in GICs to specific features of the geomagnetic storm using, for instance, geomagnetic indices, but, unfortunately, they have not produced conclusive results. Therefore, from the point of view of the possibility of understanding which SWE events are most effective in producing effects on the infrastructures, the opportunity to have a thorough characterisation of the multitude of phenomena occurring between the Sun and Earth as a consequence of a CME represents a novel, comprehensive, and promising approach. In the framework of WP1710, the GIC index [127] is obtained with data from ground geomagnetic observatories and is equipped with a risk scale [128] that provides a risk level (that becomes an alert level when real-time data are available). Moreover, with observatories aligned on a latitudinal chain, it is possible to build a time-varying GIC index latitudinal profile [129] that is helpful for monitoring the value of the magnetic latitude, which can be considered as a sort of safety threshold (i.e., countries below this threshold can be considered safe from damages due to GICs). In addition, a comparison between the GIC index and the geoelectric field estimated by means of the MA.I.GIC. model is performed in synergy with WP1420. Moreover, the global occurrence of LoL events is identified by using total electron content measurements carried out by LEO satellites.

Measuring, understanding, and characterising the SEP radiation environment inside a space habitat is mandatory for developing proper countermeasures to mitigate crew radiation risks. These measurements allow for a detailed assessment of the dose due to the solar events absorbed by the crew, and also permit a fruitful comparison with the dynamic of the outside SEP radiation field as measured by other detectors outside the space habitat and/or on satellites (as in WP1210), with the aim of building a successful 'SEP now-casting'

strategy. Therefore, data from several detectors inside the International Space Station (e.g., ALTEA, LIDAL) are being properly formatted. Radiation flux and consequent dose rates will be derived.

To showcase the proposed multidisciplinary approach, well-observed "target SWE events", exhibiting strong or moderate characteristics from several perspectives, will be studied in detail. This choice is based on the big flare syndrome [130], for which big flares have more of everything, e.g., greater SXR peak intensities, major SEP events, faster CMEs, and presumably geomagnetic storms as a consequence.

The target SWE events are of two types (possibly intersecting), which we term geoeffective and widespread (i.e., recorded at multiple heliospheric locations). The study of geoeffective events, i.e., those presenting important geomagnetic and ionospheric storms, along with CMEs, flares, and SEP events, will allow us to cover all of the aspects of SWE events in the different application domains from the Sun to Earth. The target SWE events are being identified during the project. Possible candidates are the 2003 Halloween events [131], the September 2017 events [132], the August 2018 [133], and the October 2021 events. Depending on the planets' positions, data availability, and event characteristics, the geoeffective target events could also be observed at other heliospheric locations. Indeed, the 28 October 2003 Halloween event is one of the most severe SWE events experienced by Mars in the last twenty years [134], whereas the 10 September 2017 solar flare strongly affected the composition and density of Mars' thermosphere [135]. Moreover, a set of widespread target events [136], e.g., involving fast and wide CMEs, will be analysed to address interplanetary space studies and PSW.

An efficient counteraction to the entirety of harmful SWE phenomena would require reliable forecasting methods to predict their occurrence and mitigate their impacts. Thus, CAESAR also performs the following activities: preliminary studies for the development of innovative ML methods and validation of existing ones for forecasting flares, SEP events, and Sym-H index behaviour [29,137]; the real-time monitoring of the solar, interplanetary, and magnetospheric–ionospheric conditions; and a definition of alert levels for flares, SEPs, geomagnetic storms, and GICs.

4. ASPIS Prototype

The ASPIS prototype implementation will hinge on three main pillars: the DB, the interface, and the metadata map. The three HL WPs of NODE 2000 (WP2100, WP 2200, and WP2300; see Figure 3) are each devoted to one of the pillars.

The ASPIS DB will contain mainly proprietary/co-proprietary products (see next section), with their relative data policy in a homogeneous, standardised collection of resources. Other important external data shall be accessed through links to existent archives.

We will design and realise the ASPIS DB to match the DB content, taking into consideration the prerequisites, the inputs, and the outputs of the methods and models in particular. The archive products (seen as resources) described and mapped by WP2310 and WP2320 will provide the basis for the internal structure of the ASPIS DB (designed by WP2110, implemented by WP2120, and, with the actual product ingestion, managed by WP2130).

Product specification and metadata will be flanked by the interface requirements (from WP2220 and WP2230) in the preparation of the ingestion process and of the services and tools used to access the database. The metadata database, model listings, and method listings may link and index bulk datasets and other external resources. The ASPIS application programming interface (API, developed by WP2210) will define the common set of protocols to access/submit data to the DB, allowing for both data ingestion and query. The web graphical user interface (GUI, WP2220) aims to provide easy user-friendly access to the DB. The GUI will access the DB using a set of dedicated APIs, who will act as middle-ware to the queries and provide tools (delivered by NODE1000 WPs) for a quick visualisation and analysis of the retrieved products. A possible landing page of the Web GUI would include one or more specific panels representing the near-real-time (NRT) values of relevant ASPIS data-sets, allowing for a live monitoring of the solar-terrestrial conditions.

The Web GUI will be realised to respond to the user's requests both in synchronous and asynchronous modes. While in the synchronous mode, the user can immediately access, view, and analyse the results. In the asynchronous mode the job will be run in the background and the system will send the user a message to notify the activity, with information on the job and links to retrieve the results once the computation is completed. However, users will be encouraged to implement heavy computations and advanced data handling using ASPIS.py. The ASPIS.py module (WP2230) is a library of functions in Python that provides a friendly data analysis environment to ASPIS users. This ASPIS.py module will be available for download and installation on the users' personal computers, but could also be used in online virtualisation solutions (e.g., server-side Python Notebooks). It will include modules to access the data in the ASPIS DB, plus the whole range of methods for visualisation and analysis, plus the models provided by NODE1000 WPs. We envisage that, similarly to other Python libraries (e.g., Sunpy https://sunpy.org/ (accessed on 1 October 2022) [138]) very much appreciated by the scientific community, it will ease the access and use of the products collected in ASPIS. Indeed, it is reasonable that the ASPIS.py module will build upon and extend existing relevant Python libraries, such as Astropy (https://www.astropy.org/ (accessed on 1 October 2022) [139]) or Sunpy itself. These projects already provide a broad ecosystem of inter-operable Python packages, markedly created to analyse data in the astrophysics and heliophysics domains, which also include models to compare and interpret the data. Astropy (and later Sunpy) has set a new standard on how to obtain and analyse data. The rapid ascent in popularity of these Python packages is probably due to the combination of support (in term of documentation and use case examples), the open-source approach, and rapid development, both professional and community-driven. Learning from these successful experiences, we will realise ASPIS.py, the Web GUI, and the DB content (the ASPIS archive as a whole) to be as easy as possible to reach, use, and maintain for both the developer and the users. Consequently, we will create a wiki-like documentation structure (realised by WP2330). This wiki will store and present the component and interface of ASPIS to ease its running, maintenance, and further extension, and all of the documentation created by CAESAR in the development of the APIs, the Web GUI, and the ASPIS.py module. All of the functional components of the ASPIS prototype are shown in Figure 5. Referring to this high-level scheme, we can briefly explain the ASPIS architecture and the various interactions between the WPs to build the ASPIS prototype. The NODE1000 Scientific WPs provide (red arrows in Figure 5): metadata, data, models, and methods used to populate the ASPIS DB; information on requisites for the web GUI and ASPIS.py module functionalities; and product specification and metadata. Product metadata descriptions are based on a template (black dashed arrow in Figure 5) provided by WP2310. ASPIS.py and Web GUI actions performed upon user request (query, visualisation, download, and so on) will leverage (black arrows in Figure 5) the ASPIS DB interface APIs to the ASPIS DB. Web GUI services might rely on ASPIS.py methods to perform their tasks. All metadata, data, models, methods, and specifications, as well as the DB structure, tool descriptions, and module documentation will be continuously fed (purple arrows in Figure 5) to the ASPIS Wiki. Two user categories are foreseen: researchers (advanced users), who will take full advantage of the ASPIS functionalities through both the Web application and the ASPIS.py, and general users, who are expected to mainly exploit the Web GUI functionalities.

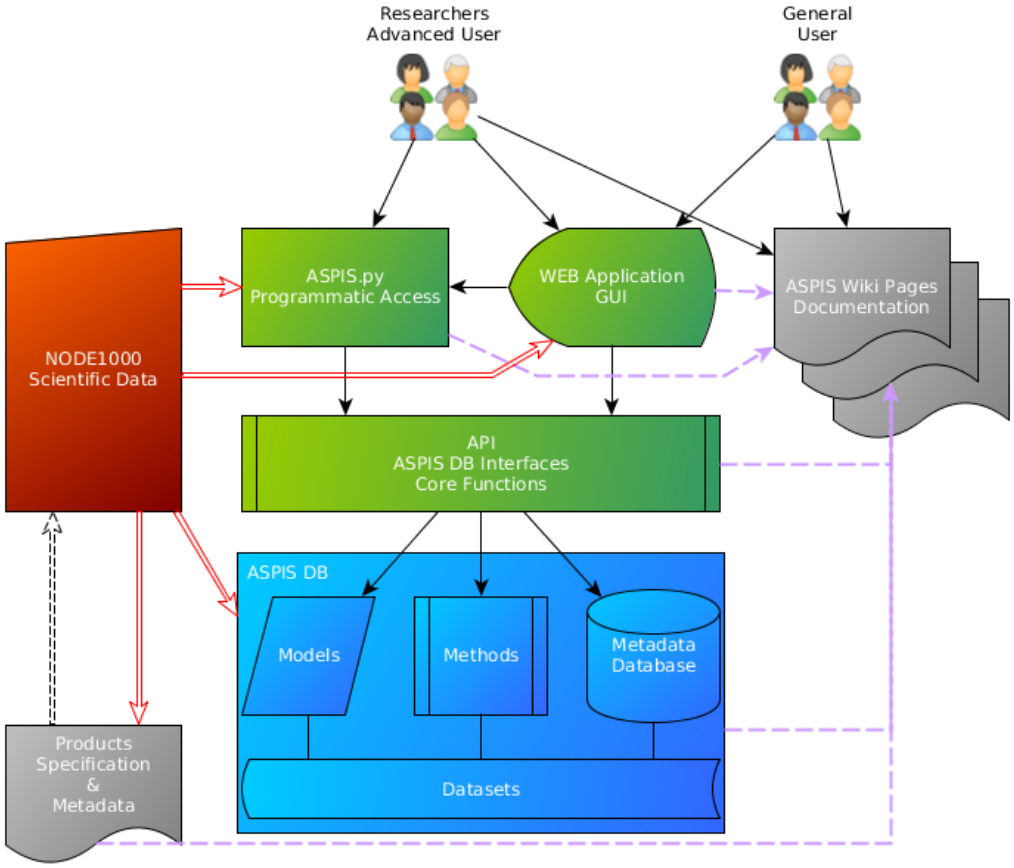

Figure 5. ASPIS high-level architecture (see the text).

ASPIS Products

Several types of proprietary/co-proprietary products will be present in the ASPIS prototype, which can be classified into four main categories: calibrated data, derived data, models, and near-real time data and tools. A summary of the intended main products for each one is provided in the following.

1. Calibrated data:
    - Full-disk LoS magnetic and velocity maps from Tor Vergata Synoptic Solar Telescope (TSST) [140];
    - H-alpha images from the TSST [141];
    - Solar Wind Analyser/Solar Orbiter data;
    - Swarm LEO satellite data;
    - CSES LEO satellite data [142];
    - Low-Frequency Array (LOFAR) radio flux;
    - Sodium exospheric data of Mercury [143,144];
    - Data from Alpha Magnetic Spectrometer (AMS) and Payload for Antimatter Matter Exploration and Light-nuclei (PAMELA);
    - Anomalous Long Term Effects on Astronauts (ALTEA) and Light Ions Detector (LIDAL) data and dose rates;
2. Derived data:
    - Features of active regions and probability of flare occurrence;
    - Catalogue of flares, SEPs, geoeffective CMEs, and ESP-associated shocks;
    - Parameters and features of interplanetary shocks, solar wind streams, magnetosheath, magnetosphere, and ionosphere;
    - SEPs properties and transport parameters at several heliographic locations;

- Time series and global maps of the magnetospheric and ionospheric origin field at ground, and of the induced geoelectric field at ground from the (Magnetospheric–Ionospheric–Geomagnetically Induced current (MA.I.GIC., [105]) model;
- Ionospheric maps and indices;
- GCR properties and propagation parameters;
- GPS LoL events maps;
- GIC index and level alert for Italy and along arrays of selected geomagnetic observatories;
- Output of test particle simulations for GCRs;

3. Models:
   - Computational methods for desaturation of EUV images;
   - Computational method for image reconstruction from Fourier X-ray data;
   - AI methods for flare prediction [25,28];
   - Computational methods for detection and tracking of global EUV waves;
   - P-drag-based model for CME propagation [59,60];
   - Ionospheric and magnetospheric current systems using TS04 model and ground magnetometer observations and applying the technique described in Piersanti and Villante [145];
   - Simulations of MHD instabilities;
   - Magnetospheric precipitation model [107];
   - Exospheric model [146];
4. Near-real-time data and tools:
   - Automated detection of AR features;
   - Geomagnetic ground-based observations;
   - Forecasting model of the SYM-H geomagnetic index;
   - Values of the equatorial plasma mass density in the inner magnetosphere updated every 15 min;
   - Ionospheric physical parameters from ionosonde;
   - Rome and Testa Grigia cosmic-ray detector data;

ASPIS will also contain publicly available external data sources such as solar images from SDO, LASCO, X-rays and particle flux data from GOES, among others.

The ASPIS prototype will be deployed in the ASI space science data centre (SSDC), will contain more than 100 products, and will be ready to ingest new additional ones. The ASPIS prototype is foreseen to be delivered by early 2024 (ASPIS logo in Figure 6).

Figure 6. ASPIS logo. Credits to Carmelo Magnafico.

5. CAESAR Dissemination Plan

One of the goals of this project is to ensure an efficient dissemination of the achieved results to maximise both the research impact and the ASPIS data exploitation. We aim to reach the scientific international community and SWE users, the educational sector, and the general public. Dissemination used to match the first group will be through publications in peer-reviewed scientific journals and via communications to scientific

conferences, symposia, meetings, and workshops. In particular, the project results will also be spread to the second group through participation in space weather-oriented events such as the European Space Weather Week (ESWW) and the European Geophysical Union (EGU). For instance, we envisage participation in an ESWW with a stand that will show the analysis performed for one target SWE event and the related data and modelling developed in CAESAR.

The educational sector will be reached through participation in national meetings of the physical, geophysical, and astronomical societies, as well as seminars and classes dedicated to the topic of this project. A virtual ASPIS event open to schools and a short presentation for high-education students will be organised.

Communication activity will be continued through the advertising of the project via scientific media and participation to the Italian edition of European Researchers' Night 2023 with a stand that will facilitate the public to get familiar with SWE events. Organising an art contest and a live event to bring the public closer to SWE researchers is also planned. The public will be asked to send images, videos, or any artwork on space-weather-related topics. The winning artworks or performances will be shared via the ASPIS website and will be used to inspire young people in space weather activities.

The CAESAR website is already available online (https://caesar.iaps.inaf.it/ (since 1 April 2022)), providing a description of the project goals and concept of the ASPIS prototype. It is periodically updated with news, headlines, and reports on developments in research and communication activities.

6. Conclusions

CAESAR is an ambitious project dedicated to synergistic investigations in all scientific fields related to space weather. It involves a wide Italian team coordinated by the INAF/Institute of Space Astrophysics and Planetology and adopts a multidisciplinary scientific approach toward studying SWE events, from their generation on the Sun to propagation in the interplanetary space, as well as the effects on Earth and planetary environments and GCR modulation.

CAESAR will also unify and harmonise the available Italian resources into the ASPIS scientific data center prototype in order to benefit a broad audience of space weather users, thus widely increasing the value of the CAESAR project. ASPIS will have a flexible architecture to allow users to perform advanced scientific studies for SWE easily and directly both through the web interface and a dedicated downloadable application called ASPIS.py. The analysis of the ASPIS data is expected to produce a significant scientific outcome in the field of space weather. In particular, the expected return from CAESAR scientific activities is likely to provide new insights toward SWE science and also stimulate further synergistic approaches at international level. Moreover, the interdisciplinary data analyses within CAESAR are expected to produce significant results to benefit international efforts aiming at transitioning the state-of-the-art physics-based models to operational use.

As an unrestricted flow of data across geo-political and organisational boundaries is needed, the ASPIS scientific centre will join the international infrastructures in being exploited by the whole SWE community and will significantly contribute to the overall progress in SWE science.

Author Contributions: Conceptualisation, M.L. and D.D.M.; methodology, M.L. and D.D.M.; writing—original draft preparation, M.L.; writing—review and editing, all authors; project management, M.L. All authors have read and agreed to the published version of the manuscript.

Funding: This research was funded by Agenzia Spaziale Italiana and Istituto Nazionale di Astrofisica grant agreement ASI-INAF n.2020-35-HH.0.

Data Availability Statement: Not applicable.

Acknowledgments: CAESAR is supported by the Italian Space Agency and the National Institute of Astrophysics through the ASI-INAF n.2020-35-HH.0 agreement for the development of the ASPIS

prototype of scientific data centre for Space Weather. N.T. acknowledges the support from ASI through the ASI-Unipg agreement 2019-2-HH.0.

Conflicts of Interest: The authors declare no conflict of interest.

References

1. Opgenoorth, H.J.; Wimmer-Schweingruber, R.F.; Belehaki, A.; Berghmans, D.; Hapgood, M.; Hesse, M.; Kauristie, K.; Lester, M.; Lilensten, J.; Messerotti, M.; et al. Assessment and recommendations for a consolidated European approach to space weather—As part of a global space weather effort. *J. Space Weather Space Clim.* **2019**, *9*, A37. [CrossRef]
2. Lilensten, J.; Belehaki, A. Developing the scientific basis for monitoring, modelling and predicting space weather. *Acta Geophys.* **2009**, *57*, 1–14. [CrossRef]
3. Plainaki, C.; Lilensten, J.; Radioti, A.; Andriopoulou, M.; Milillo, A.; Nordheim, T.A.; Dandouras, I.; Coustenis, A.; Grassi, D.; Mangano, V.; et al. Planetary space weather: Scientific aspects and future perspectives. *J. Space Weather Space Clim.* **2016**, *6*, A31. [CrossRef]
4. Bentley, R.; Csillaghy, A.; Aboudarham, J.; Jacquey, C.; Hapgood, M.; Bocchialini, K.; Messerotti, M.; Brooke, J.; Gallagher, P.; Fox, P.; et al. Helio: The heliophysics integrated observatory. *Adv. Space Res.* **2011**, *47*, 2235–2239. [CrossRef]
5. Aboudarham, J.; Bentley, R.; Csillaghy, A.; Jacquey, C.; Richards, P.; Bocchialini, K.; Messerotti, M.; Brooke, J.; Gallagher, P.; Roberts, A.; et al. *HELIO, a Powerful Tool for Space Weather Science*; BASS2000; European Commission: Brussels, Belgium, 2013.
6. Bentley, R.; Lapenta, G.; Blanc, M.; Fox, P.; Walker, R.; Team, C. VOs and Heliophysics: Would anyone like some CASSIS? In *Proceedings of the AGU Fall Meeting Abstracts*; IN23B-1358; American Geophysical Union: Washington, DC, USA, 2010; Volume 2010.
7. Clette, F. Past and future sunspot indices: New goals for SoTerIA. *J. Atmos. Sol.-Terr. Phys.* **2011**, *73*, 182–186. [CrossRef]
8. Harrison, R.; Davies, J.; Perry, C.; Moestl, C.; Rouillard, A.; Bothmer, V.; Rodriguez, L.; Eastwood, J.; Kilpua, E.; Gallagher, P.; et al. Overview of the HELCATS project. In Proceedings of the EGU General Assembly Conference Abstracts, Vienna, Austria, 23–28 April 2017; p. 5296.
9. Malandraki, O.; Klein, K.L.; Vainio, R.; Agueda, N.; Núñez, M.; Heber, B.; Bütikofer, R.; Sarlanis, C.; Crosby, N.; Share, G.; et al. High energy solar particle events forecasting and analysis: The HESPERIA project. In Proceedings of the 34th International Cosmic Ray Conference ICRC 2015, The Hague, The Netherlands, 30 July–6 August 2015.
10. Plainaki, C.; Antonucci, M.; Bemporad, A.; Berrilli, F.; Bertucci, B.; Castronuovo, M.; De Michelis, P.; Giardino, M.; Iuppa, R.; Laurenza, M.; et al. Current state and perspectives of Space Weather science in Italy. *J. Space Weather Space Clim.* **2020**, *10*, 6. [CrossRef]
11. Abramenko, V.I.; Carbone, V.; Yurchyshyn, V.; Goode, P.R.; Stein, R.F.; Lepreti, F.; Capparelli, V.; Vecchio, A. Turbulent Diffusion in the Photosphere as Derived from Photospheric Bright Point Motion. *Astrophys. J.* **2011**, *743*, 133. [CrossRef]
12. Vecchio, A.; Laurenza, M.; Meduri, D.; Carbone, V.; Storini, M. The Dynamics of the Solar Magnetic Field: Polarity Reversals, Butterfly Diagram, and Quasi-Biennial Oscillations. *Astrophys. J.* **2012**, *749*, 27. [CrossRef]
13. Lepreti, F.; Carbone, V.; Abramenko, V.I.; Yurchyshyn, V.; Goode, P.R.; Capparelli, V.; Vecchio, A. Turbulent Pair Dispersion of Photospheric Bright Points. *Astrophys. J. Lett.* **2012**, *759*, L17. [CrossRef]
14. Giannattasio, F.; Consolini, G.; Berrilli, F.; Del Moro, D. The Complex Nature of Magnetic Element Transport in the Quiet Sun: The Lévy-walk Character. *Astrophys. J.* **2019**, *878*, 33. [CrossRef]
15. Giannattasio, F.; Consolini, G. The Complex Nature of Magnetic Element Transport in the Quiet Sun: The Multiscaling Character. *Astrophys. J.* **2021**, *908*, 142. [CrossRef]
16. Cauzzi, G.; Reardon, K.P.; Uitenbroek, H.; Cavallini, F.; Falchi, A.; Falciani, R.; Janssen, K.; Rimmele, T.; Vecchio, A.; Wöger, F. The solar chromosphere at high resolution with IBIS. I. New insights from the Ca II 854.2 nm line. *Astron. Astrophys.* **2008**, *480*, 515–526. [CrossRef]
17. Reardon, K.P.; Lepreti, F.; Carbone, V.; Vecchio, A. Evidence of Shock-driven Turbulence in the Solar Chromosphere. *Astrophys. J. Lett.* **2008**, *683*, L207,
18. Forbes, T.G. A review on the genesis of coronal mass ejections. *J. Geophys. Res.* **2000**, *105*, 23153–23166. [CrossRef]
19. Aschwanden, M.J. Particle acceleration and kinematics in solar flares—A Synthesis of Recent Observations and Theoretical Concepts (Invited Review). *Space Sci. Rev.* **2002**, *101*, 1–227. [CrossRef]
20. Temmer, M. Space weather: The solar perspective. *Living Rev. Sol. Phys.* **2021**, *18*, 4, [CrossRef]
21. Romano, P.; Zuccarello, F. Flare occurrence and the spatial distribution of the magnetic helicity flux. *Astron. Astrophys.* **2011**, *535*, A1. [CrossRef]
22. Zuccarello, F.; Balmaceda, L.; Cessateur, G.; Cremades, H.; Guglielmino, S.L.; Lilensten, J.; Dudok de Wit, T.; Kretzschmar, M.; Lopez, F.M.; Mierla, M.; et al. Solar activity and its evolution across the corona: Recent advances. *J. Space Weather Space Clim.* **2013**, *3*, A18. [CrossRef]
23. Laurenza, M.; Consolini, G.; Storini, M.; Damiani, A. The Weibull functional form for SEP event spectra. *J. Phys. Conf. Ser.* **2015**, *632*, 012066. [CrossRef]
24. Frassati, F.; Laurenza, M.; Bemporad, A.; West, M.J.; Mancuso, S.; Susino, R.; Alberti, T.; Romano, P. Acceleration of Solar Energetic Particles through CME-driven Shock and Streamer Interaction. *Astrophys. J.* **2022**, *926*, 227. [CrossRef]

25. Cicogna, D.; Berrilli, F.; Calchetti, D.; Del Moro, D.; Giovannelli, L.; Benvenuto, F.; Campi, C.; Guastavino, S.; Piana, M. Flare-forecasting Algorithms Based on High-gradient Polarity Inversion Lines in Active Regions. *Astrophys. J.* **2021**, *915*, 38. [CrossRef]
26. Laurenza, M.; Cliver, E.W.; Hewitt, J.; Storini, M.; Ling, A.G.; Balch, C.C.; Kaiser, M.L. A technique for short-term warning of solar energetic particle events based on flare location, flare size, and evidence of particle escape. *Space Weather* **2009**, *7*, S04008. [CrossRef]
27. Laurenza, M.; Alberti, T.; Cliver, E.W. A Short-term ESPERTA-based Forecast Tool for Moderate-to-extreme Solar Proton Events. *Astrophys. J.* **2018**, *857*, 107. [CrossRef]
28. Campi, C.; Benvenuto, F.; Massone, A.M.; Bloomfield, D.S.; Georgoulis, M.K.; Piana, M. Feature Ranking of Active Region Source Properties in Solar Flare Forecasting and the Uncompromised Stochasticity of Flare Occurrence. *Astrophys. J.* **2019**, *883*, 150. [CrossRef]
29. Stumpo, M.; Benella, S.; Laurenza, M.; Alberti, T.; Consolini, G.; Marcucci, M.F. Open Issues in Statistical Forecasting of Solar Proton Events: A Machine Learning Perspective. *Space Weather* **2021**, *19*, e02794. [CrossRef]
30. Wang, H. Evolution of vector magnetic fields and the August 27 1990 X-3 flare. *Sol. Phys.* **1992**, *140*, 85–98. [CrossRef]
31. Toriumi, S.; Wang, H. Flare-productive active regions. *Living Rev. Sol. Phys.* **2019**, *16*, 3. [CrossRef] [PubMed]
32. Vasantharaju, N.; Vemareddy, P.; Ravindra, B.; Doddamani, V.H. Magnetic Imprints of Eruptive and Noneruptive Solar Flares as Observed by Solar Dynamics Observatory. *Astrophys. J.* **2022**, *927*, 86, [CrossRef]
33. Cliver, E.W.; Laurenza, M.; Storini, M.; Thompson, B.J. On the Origins of Solar EIT Waves. *Astrophys. J.* **2005**, *631*, 604–611. [CrossRef]
34. West, M.J.; Seaton, D.B.; D'Huys, E.; Mierla, M.; Laurenza, M.; Meyer, K.A.; Berghmans, D.; Rachmeler, L.R.; Rodriguez, L.; Stegen, K. A Review of the Extended EUV Corona Observed by the Sun Watcher with Active Pixels and Image Processing (SWAP) Instrument. *Sol. Phys.* **2022**, *297*, 136. [CrossRef]
35. Gopalswamy, N.; Yashiro, S.; Akiyama, S. Kinematic and Energetic Properties of the 2012 March 12 Polar Coronal Mass Ejection. *Astrophys. J.* **2015**, *809*, 106, [CrossRef]
36. Odstrcil, D. Modeling 3-D solar wind structure. *Adv. Space Res.* **2003**, *32*, 497–506. [CrossRef]
37. Cargill, P.J. On the Aerodynamic Drag Force Acting on Interplanetary Coronal Mass Ejections. *Sol. Phys.* **2004**, *221*, 135–149. [CrossRef]
38. Pomoell, J.; Poedts, S. EUHFORIA: European heliospheric forecasting information asset. *J. Space Weather Space Clim.* **2018**, *8*, A35. [CrossRef]
39. Cane, H.V.; Richardson, I.G.; St. Cyr, O.C. Coronal mass ejections, interplanetary ejecta and geomagnetic storms. *Geophys. Res. Lett.* **2000**, *27*, 3591–3594. [CrossRef]
40. Aran, A.; Lario, D.; Sanahuja, B.; Marsden, R.G.; Dryer, M.; Fry, C.D.; McKenna-Lawlor, S.M.P. Modeling and forecasting solar energetic particle events at Mars: The event on 6 March 1989. *Astron. Astrophys.* **2007**, *469*, 1123–1134. [CrossRef]
41. Vainio, R.; Desorgher, L.; Heynderickx, D.; Storini, M.; Flückiger, E.; Horne, R.B.; Kovaltsov, G.A.; Kudela, K.; Laurenza, M.; McKenna-Lawlor, S.; et al. Dynamics of the Earth's Particle Radiation Environment. *Space Sci. Rev.* **2009**, *147*, 187–231. [CrossRef]
42. Diego, P.; Storini, M.; Parisi, M.; Cordaro, E.G. AE index variability during corotating fast solar wind streams. *J. Geophys. Res. Space Phys.* **2005**, *110*, A06105. [CrossRef]
43. D'Amicis, R.; Bruno, R.; Bavassano, B. Is geomagnetic activity driven by solar wind turbulence? *Geophys. Res. Lett.* **2007**, *34*, L05108. [CrossRef]
44. Lario, D.; Ho, G.C.; Decker, R.B.; Roelof, E.C.; Desai, M.I.; Smith, C.W. ACE Observations of Energetic Particles Associated with Transient Interplanetary Shocks. *AIP Conf. Proc.* **2003**, *679*, 640–643. [CrossRef]
45. Kallenrode, M.B. A statistical survey of 5-MeV proton events at transient interplanetary shocks. *J. Geophys. Res.* **1996**, *101*, 24393–24410. [CrossRef]
46. Perri, S.; Zimbardo, G. Superdiffusive transport of electrons accelerated at corotating interaction regions. *J. Geophys. Res. (Space Phys.)* **2008**, *113*, A03107. [CrossRef]
47. Dresing, N.; Theesen, S.; Klassen, A.; Heber, B. Efficiency of particle acceleration at interplanetary shocks: Statistical study of STEREO observations. *Astron. Astrophys.* **2016**, *588*, A17, [CrossRef]
48. Laurenza, M.; Consolini, G.; Storini, M.; Pallocchia, G.; Damiani, A. The Weibull functional form for the energetic particle spectrum at interplanetary shock waves. *J. Phys. Conf. Ser.* **2016**, *767*, 012015. [CrossRef]
49. Pallocchia, G.; Laurenza, M.; Consolini, G. On Weibull's Spectrum of Non-relativistic Energetic Particles at IP Shocks: Observations and Theoretical Interpretation. *Astrophys. J.* **2017**, *837*, 158. [CrossRef]
50. Chiappetta, F.; Laurenza, M.; Lepreti, F.; Consolini, G. Proton Energy Spectra of Energetic Storm Particle Events and Relation with Shock Parameters and Turbulence. *Astrophys. J.* **2021**, *915*, 8. [CrossRef]
51. Perri, S.; Bykov, A.; Fahr, H.; Fichtner, H.; Giacalone, J. Recent Developments in Particle Acceleration at Shocks: Theory and Observations. *Space Sci. Rev.* **2022**, *218*, 26. [CrossRef]
52. Fox, N.J.; Velli, M.C.; Bale, S.D.; Decker, R.; Driesman, A.; Howard, R.A.; Kasper, J.C.; Kinnison, J.; Kusterer, M.; Lario, D.; et al. The Solar Probe Plus Mission: Humanity's First Visit to Our Star. *Space Sci. Rev.* **2016**, *204*, 7–48. [CrossRef]
53. Müller, D.; St. Cyr, O.C.; Zouganelis, I.; Gilbert, H.R.; Marsden, R.; Nieves-Chinchilla, T.; Antonucci, E.; Auchère, F.; Berghmans, D.; Horbury, T.S.; et al. The Solar Orbiter mission. Science overview. *Astron. Astrophys.* **2020**, *642*, A1, [CrossRef]

54. Benkhoff, J.; Murakami, G.; Baumjohann, W.; Besse, S.; Bunce, E.; Casale, M.; Cremosese, G.; Glassmeier, K.H.; Hayakawa, H.; Heyner, D.; et al. BepiColombo—Mission Overview and Science Goals. *Space Sci. Rev.* **2021**, *217*, 90. [CrossRef]
55. Borovsky, J.E. A Statistical Analysis of the Fluctuations in the Upstream and Downstream Plasmas of 109 Strong-Compression Interplanetary Shocks at 1 AU. *J. Geophys. Res. Space Phys.* **2020**, *125*, e2019JA027518. [CrossRef]
56. Pitňa, A.; Šafránková, J.; Němeček, Z.; Ďurovcová, T.; Kis, A. Turbulence Upstream and Downstream of Interplanetary Shocks. *Front. Phys.* **2021**, *8*, 626768. [CrossRef]
57. Tsurutani, B.T.; Gonzalez, W.D. The cause of high-intensity long-duration continuous AE activity (HILDCAAs): Interplanetary Alfvén wave trains. *Planet. Space Sci.* **1987**, *35*, 405–412. [CrossRef]
58. Telloni, D.; D'Amicis, R.; Bruno, R.; Perrone, D.; Sorriso-Valvo, L.; Raghav, A.N.; Choraghe, K. Alfvénicity-related Long Recovery Phases of Geomagnetic Storms: A Space Weather Perspective. *Astrophys. J.* **2021**, *916*, 64. [CrossRef]
59. Napoletano, G.; Forte, R.; Del Moro, D.; Pietropaolo, E.; Giovannelli, L.; Berrilli, F. A probabilistic approach to the drag-based model. *J. Space Weather Space Clim.* **2018**, *8*, A11, [CrossRef]
60. Del Moro, D.; Napoletano, G.; Forte, R.; Giovannelli, L.; Pietropaolo, E.; Berrilli, F. Forecasting the 2018 February 12th CME propagation with the P-DBM model: A fast warning procedure. *Ann. Geophys.* **2019**, *62*, GM456. [CrossRef]
61. Napoletano, G.; Foldes, R.; Camporeale, E.; de Gasperis, G.; Giovannelli, L.; Paouris, E.; Pietropaolo, E.; Teunissen, J.; Tiwari, A.K.; Del Moro, D. Parameter Distributions for the Drag-Based Modeling of CME Propagation. *Space Weather* **2022**, *20*, e2021SW002925. [CrossRef]
62. Hu, Q.; Sonnerup, B.U.O. Reconstruction of magnetic clouds in the solar wind: Orientations and configurations. *J. Geophys. Res. Space Phys.* **2002**, *107*, SSH 10-1–SSH 10-15, [CrossRef]
63. Hu, Q. The Grad-Shafranov reconstruction in twenty years: 1996–2016. *Sci. China Earth Sci.* **2017**, *60*, 1466–1494. [CrossRef]
64. Benella, S.; Laurenza, M.; Vainio, R.; Grimani, C.; Consolini, G.; Hu, Q.; Afanasiev, A. A New Method to Model Magnetic Cloud-driven Forbush Decreases: The 2016 August 2 Event. *Astrophys. J.* **2020**, *901*, 21. [CrossRef]
65. Pulkkinen, T. Space Weather: Terrestrial Perspective. *Living Rev. Sol. Phys.* **2007**, *4*, 1. [CrossRef]
66. Consolini, G.; De Michelis, P.; Tozzi, R. On the Earth's magnetospheric dynamics: Nonequilibrium evolution and the fluctuation theorem. *J. Geophys. Res. Space Phys.* **2008**, *113*. [CrossRef]
67. De Michelis, P.; Consolini, G.; Tozzi, R.; Marcucci, M.F. Observations of high-latitude geomagnetic field fluctuations during St. Patrick's Day storm: Swarm and SuperDARN measurements. *Earth Planets Space* **2016**, *68*, 105. [CrossRef]
68. Alberti, T.; Giannattasio, F.; De Michelis, P.; Consolini, G. Linear Versus Nonlinear Methods for Detecting Magnetospheric and Ionospheric Current Systems Patterns. *Earth Space Sci.* **2020**, *7*, e00559. [CrossRef]
69. Santarelli, L.; De Michelis, P.; Consolini, G. Hints on the Multiscale Nature of Geomagnetic Field Fluctuations During Quiet and Disturbed Periods. *J. Geophys. Res. (Space Phys.)* **2021**, *126*, e28596. [CrossRef]
70. Piersanti, M.; Del Moro, D.; Parmentier, A.; Martucci, M.; Palma, F.; Sotgiu, A.; Plainaki, C.; D'Angelo, G.; Berrilli, F.; Recchiuti, D.; et al. On the Magnetosphere-Ionosphere Coupling During the May 2021 Geomagnetic Storm. *Space Weather* **2022**, *20*, e2021SW003016, [CrossRef]
71. Alberti, T.; Faranda, D.; Consolini, G.; De Michelis, P.; Donner, R.V.; Carbone, V. Concurrent Effects between Geomagnetic Storms and Magnetospheric Substorms. *Universe* **2022**, *8*, 226. [CrossRef]
72. Marcucci, M.F.; Coco, I.; Ambrosino, D.; Amata, E.; Milan, S.E.; Bavassano Cattaneo, M.B.; Retinò, A. Extended SuperDARN and IMAGE observations for northward IMF: Evidence for dual lobe reconnection. *J. Geophys. Res. (Space Phys.)* **2008**, *113*, A02204. [CrossRef]
73. Hasegawa, H.; Fujimoto, M.; Phan, T.D.; Rème, H.; Balogh, A.; Dunlop, M.W.; Hashimoto, C.; TanDokoro, R. Transport of solar wind into Earth's magnetosphere through rolled-up Kelvin-Helmholtz vortices. *Nature* **2004**, *430*, 755–758. [CrossRef]
74. Liemohn, M.W. Introduction to special section on "Results of the National Science Foundation Geospace Environment Modeling Inner Magnetosphere/Storms Assessment Challenge". *J. Geophys. Res. (Space Phys.)* **2006**, *111*, A11S01. [CrossRef]
75. Thorne, R.M. Radiation belt dynamics: The importance of wave-particle interactions. *Geophys. Res. Lett.* **2010**, *37*. [CrossRef]
76. Eastwood, J.P.; Nakamura, R.; Turc, L.; Mejnertsen, L.; Hesse, M. The Scientific Foundations of Forecasting Magnetospheric Space Weather. *Space Sci. Rev.* **2017**, *212*, 1221–1252. [CrossRef]
77. Sharma, A.S.; Kamide, Y.; Lakhina, G.S. Disturbances on geospace: The storm-substorm relationship. *Geophys. Monogr.* **2003**, *142*. [CrossRef]
78. Raeder, J.; Larson, D.; Li, W.; Kepko, E.L.; Fuller-Rowell, T. OpenGGCM Simulations for the THEMIS Mission. *Space Sci. Rev.* **2008**, *141*, 535–555. [CrossRef]
79. Paschmann, G.; Sonnerup, B.U.O.; Papamastorakis, I.; Sckopke, N.; Haerendel, G.; Bame, S.J.; Asbridge, J.R.; Gosling, J.T.; Russell, C.T.; Elphic, R.C. Plasma acceleration at the Earth's magnetopause: Evidence for reconnection. *Nature* **1979**, *282*, 243–246. [CrossRef]
80. Sonnerup, B.U.Ö.; Haaland, S.E.; Paschmann, G.; Denton, R.E. Quality Measure for the Walén Relation. *J. Geophys. Res. (Space Phys.)* **2018**, *123*, 9979–9990. [CrossRef]
81. Tsyganenko, N.A.; Sitnov, M.I. Modeling the dynamics of the inner magnetosphere during strong geomagnetic storms. *J. Geophys. Res. Space Phys.* **2005**, *110*, A03208.

82. Lichtenberger, J.; Clilverd, M.A.; Heilig, B.; Vellante, M.; Manninen, J.; Rodger, C.J.; Collier, A.B.; Jørgensen, A.M.; Reda, J.; Holzworth, R.H.; et al. The plasmasphere during a space weather event: First results from the PLASMON project. *J. Space Weather Space Clim.* **2013**, *3*, A23. [CrossRef]
83. Del Corpo, A.; Vellante, M.; Heilig, B.; Pietropaolo, E.; Reda, J.; Lichtenberger, J. Observing the cold plasma in the Earth's magnetosphere with the EMMA network. *Ann. Geophys.* **2019**, *62*, GM447. [CrossRef]
84. Del Corpo, A.; Vellante, M.; Heilig, B.; Pietropaolo, E.; Reda, J.; Lichtenberger, J. An Empirical Model for the Dayside Magnetospheric Plasma Mass Density Derived From EMMA Magnetometer Network Observations. *J. Geophys. Res. Space Phys.* **2020**, *125*, e2019JA027381, [CrossRef]
85. Foldes, R.; Del Corpo, A.; Pietropaolo, E.; Vellante, M. Assessing Machine Learning Techniques for Identifying Field Line Resonance Frequencies From Cross-Phase Spectra. *J. Geophys. Res. Space Phys.* **2021**, *126*, e2020JA029008, [CrossRef]
86. De Michelis, P.; Pignalberi, A.; Consolini, G.; Coco, I.; Tozzi, R.; Pezzopane, M.; Giannattasio, F.; Balasis, G. On the 2015 St. Patrick's Storm Turbulent State of the Ionosphere: Hints From the Swarm Mission. *J. Geophys. Res. Space Phys.* **2020**, *125*, e2020JA027934, [CrossRef]
87. Pignalberi, A.; Giannattasio, F.; Truhlik, V.; Coco, I.; Pezzopane, M.; Consolini, G.; De Michelis, P.; Tozzi, R. On the Electron Temperature in the Topside Ionosphere as Seen by Swarm Satellites, Incoherent Scatter Radars, and the International Reference Ionosphere Model. *Remote Sens.* **2021**, *13*, 4077. [CrossRef]
88. Giannattasio, F.; De Michelis, P.; Pignalberi, A.; Coco, I.; Consolini, G.; Pezzopane, M.; Tozzi, R. Parallel Electrical Conductivity in the Topside Ionosphere Derived From Swarm Measurements. *J. Geophys. Res. (Space Phys.)* **2021**, *126*, e28452. [CrossRef]
89. Giannattasio, F.; Pignalberi, A.; De Michelis, P.; Coco, I.; Consolini, G.; Pezzopane, M.; Tozzi, R. Dependence of Parallel Electrical Conductivity in the Topside Ionosphere on Solar and Geomagnetic Activity. *J. Geophys. Res. (Space Phys.)* **2021**, *126*, e29138. [CrossRef]
90. Giannattasio, F.; Consolini, G.; Coco, I.; De Michelis, P.; Pezzopane, M.; Pignalberi, A.; Tozzi, R. Dissipation of field-aligned currents in the topside ionosphere. *Sci. Rep.* **2022**, *12*, 17202. [CrossRef]
91. Baskaradas, J.; Bianchi, C.; Pezzopane, M.; Romano, V.; Umberto, S.; Scotto, C.; G, T.; Zuccheretti, E. New low power pulse compressed ionosonde at Gibilmanna Ionospheric Observatory. *Ann. Geophys.* **2005**, *48*. [CrossRef]
92. Pezzopane, M.; Scotto, C. Software for the automatic scaling of critical frequency f0F2 and MUF(3000) F2 from ionograms appliedat the Ionospheric Observatory of Gibilmanna. *Ann. Geophys.* **2004**, *47*. [CrossRef]
93. Pezzopane, M.; Zuccheretti, E.; Bianchi, C.; Scotto, C.; Zolesi, B.; Cabrera, M.A.; Ezquer, R.G. The new ionospheric station of Tucuman: First results. *Ann. Geophys.* **2007**, *50*. [CrossRef]
94. Greenwald, R.A.; Baker, K.B.; Dudeney, J.R.; Pinnock, M.; Jones, T.B.; Thomas, E.C.; Villain, J.P.; Cerisier, J.C.; Senior, C.; Hanuise, C.; et al. DARN/SuperDARN. *Space Sci. Rev.* **1995**, *71*, 761–796. [CrossRef]
95. Ruohoniemi, J.M.; Baker, K.B. Large-scale imaging of high-latitude convection with Super Dual Auroral Radar Network HF radar observations. *J. Geophys. Res. Space Phys.* **1998**, *103*, 20797–20811. [CrossRef]
96. Borovsky, J.E.; Lavraud, B.; Kuznetsova, M.M. Polar cap potential saturation, dayside reconnection, and changes to the magnetosphere. *J. Geophys. Res. Space Phys.* **2009**, *114*. [CrossRef]
97. Milan, S.E.; Gosling, J.S.; Hubert, B. Relationship between interplanetary parameters and the magnetopause reconnection rate quantified from observations of the expanding polar cap. *J. Geophys. Res. Space Phys.* **2012**, *117*. [CrossRef]
98. Friis-Christensen, E.; Lühr, H.; Hulot, G. SWARM: A constellation to study the Earth's magnetic field. *Earth Planets Space* **2006**, *58*, 351–358. [CrossRef]
99. Shen, X.; Zhang, X.; Yuan, S.; Wang, L.; Cao, J.; Huang, J.; Zhu, X.; Piergiorgio, P.; Dai, J. The state-of-the-art of the China Seismo-Electromagnetic Satellite mission. *Sci. China Technol. Sci.* **2018**, *61*, 634–642. [CrossRef]
100. Pi, X.; Mannucci, A.J.; Lindqwister, U.J.; Ho, C.M. Monitoring of global ionospheric irregularities using the Worldwide GPS Network. *Geophys. Res. Lett.* **1997**, *24*, 2283–2286. [CrossRef]
101. Xiong, C.; Stolle, C.; Lühr, H. The Swarm satellite loss of GPS signal and its relation to ionospheric plasma irregularities. *Space Weather* **2016**, *14*, 563–577. [CrossRef]
102. Jin, Y.; Spicher, A.; Xiong, C.; Clausen, L.B.N.; Kervalishvili, G.; Stolle, C.; Miloch, W.J. Ionospheric Plasma Irregularities Characterized by the Swarm Satellites: Statistics at High Latitudes. *J. Geophys. Res. Space Phys.* **2019**, *124*, 1262–1282.
103. Pignalberi, A.; Coco, I.; Giannattasio, F.; Pezzopane, M.; De Michelis, P.; Consolini, G.; Tozzi, R. A New Ionospheric Index to Investigate Electron Temperature Small-Scale Variations in the Topside Ionosphere. *Universe* **2021**, *7*, 290. [CrossRef]
104. Pignalberi, A. TITIPy: A Python tool for the calculation and mapping of topside ionosphere turbulence indices. *Comput. Geosci.* **2021**, *148*, 104675. [CrossRef]
105. Piersanti, M.; Di Matteo, S.; Carter, B.A.; Currie, J.; D'Angelo, G. Geoelectric Field Evaluation During the September 2017 Geomagnetic Storm: MA.I.GIC. Model. *Space Weather* **2019**, *17*, 1241–1256. [CrossRef]
106. Ivanovski, S.; Kartalev, M.; Dobreva, P.; Vatkova, G.; Chernogorova, T. Coupled Kelvin-Helmholtz and Tearing Mode Instabilities in the Magnetopause Layer. *J. Theor. Appl. Mech.* **2011**, *41*, 31–42.
107. Massetti, S.; Orsini, S.; Milillo, A.; Mura, A. Modelling Mercury's magnetosphere and plasma entry through the dayside magnetopause. *Planet. Space Sci.* **2007**, *55*, 1557–1568. [CrossRef]
108. Kallio, E.; Janhunen, P. Solar wind and magnetospheric ion impact on Mercury's surface. *Geophys. Res. Lett.* **2003**, *30*. [CrossRef]

109. Fatemi, S.; Poppe, A.R.; Barabash, S. Hybrid Simulations of Solar Wind Proton Precipitation to the Surface of Mercury. *J. Geophys. Res. Space Phys.* **2020**, *125*, e2019JA027706, [CrossRef]
110. Slavin, J.A.; DiBraccio, G.A.; Gershman, D.J.; Imber, S.M.; Poh, G.K.; Raines, J.M.; Zurbuchen, T.H.; Jia, X.; Baker, D.N.; Glassmeier, K.H.; et al. MESSENGER observations of Mercury's dayside magnetosphere under extreme solar wind conditions. *J. Geophys. Res. Space Phys.* **2014**, *119*, 8087–8116. [CrossRef]
111. Mura, A.; Wurz, P.; Lichtenegger, H.I.; Schleicher, H.; Lammer, H.; Delcourt, D.; Milillo, A.; Orsini, S.; Massetti, S.; Khodachenko, M.L. The sodium exosphere of Mercury: Comparison between observations during Mercury's transit and model results. *Icarus* **2009**, *200*, 1–11. [CrossRef]
112. Leblanc, F.; Doressoundiram, A.; Schneider, N.; Massetti, S.; Wedlund, M.; López Ariste, A.; Barbieri, C.; Mangano, V.; Cremonese, G. Short-term variations of Mercury's Na exosphere observed with very high spectral resolution. *Geophys. Res. Lett.* **2009**, *36*. [CrossRef]
113. Potgieter, M.S. Solar Modulation of Cosmic Rays. *Living Rev. Sol. Phys.* **2013**, *10*, 3. [CrossRef]
114. Kudela, K.; Storini, M.; Hofer, M.Y.; Belov, A. Cosmic Rays in Relation to Space Weather. *Space Sci. Rev.* **2000**, *93*, 153–174. [CrossRef]
115. Vecchio, A.; Laurenza, M.; Carbone, V.; Storini, M. Quasi-Biennial Modulation of Solar Neutrino Flux and Solar and Galactic Cosmic Rays By Solar Cyclic Activity. *Astrophys. J.* **2009**, *709*, L1–L5. [CrossRef]
116. Tomassetti, N. Solar and nuclear physics uncertainties in cosmic-ray propagation. *Phys. Rev. D* **2017**, *96*, 103005. [CrossRef]
117. Laurenza, M.; Vecchio, A.; Storini, M.; Carbone, V. Drift Effects on the Galactic Cosmic Ray Modulation. *Astrophys. J.* **2014**, *781*, 71. [CrossRef]
118. Laurenza, M.; Alberti, T.; Marcucci, M.F.; Consolini, G.; Jacquey, C.; Molendi, S.; Macculi, C.; Lotti, S. Estimation of the Particle Radiation Environment at the L1 Point and in Near-Earth Space. *Astrophys. J.* **2019**, *873*, 112. [CrossRef]
119. Armano, M.; Audley, H.; Baird, J.; Bassan, M.; Benella, S.; Binetruy, P.; Born, M.; Bortoluzzi, D.; Cavalleri, A.; Cesarini, A.; et al. Characteristics and Energy Dependence of Recurrent Galactic Cosmic-Ray Flux Depressions and of a Forbush Decrease with *LISA Pathfinder*. *Astrophys. J.* **2018**, *854*, 113. [CrossRef]
120. Aguilar, M.; Cavasonza, L.A.; Ambrosi, G.; Arruda, L.; Attig, N.; Barao, F.; Barrin, L.; Bartoloni, A.; Başeğmez-du Pree, S.; Battiston, R.; et al. Periodicities in the Daily Proton Fluxes from 2011 to 2019 Measured by the Alpha Magnetic Spectrometer on the International Space Station from 1 to 100 GV. *Phys. Rev. Lett.* **2021**, *127*, 271102. [CrossRef]
121. Berrilli, F.; Casolino, M.; Del Moro, D.; Di Fino, L.; Larosa, M.; Narici, L.; Piazzesi, R.; Picozza, P.; Scardigli, S.; Sparvoli, R.; et al. The relativistic solar particle event of May 17th, 2012 observed on board the International Space Station. *J. Space Weather Space Clim.* **2014**, *4*, A16. [CrossRef]
122. Di Fino, L.; Zaconte, V.; Stangalini, M.; Sparvoli, R.; Picozza, P.; Piazzesi, R.; Narici, L.; Larosa, M.; Del Moro, D.; Casolino, M.; et al. Solar particle event detected by ALTEA on board the International Space Station. The March 7th, 2012 X5.4 flare. *J. Space Weather Space Clim.* **2014**, *4*, A19. [CrossRef]
123. Buzulukova, N. *Extreme Events in Geospace: Origins, Predictability, and Consequences*; Elsevier: Amsterdam, The Netherlands, 2017.
124. Piersanti, M.; Carter, B. Chapter 10—Geomagnetically induced currents. In *The Dynamical Ionosphere*; Materassi, M., Forte, B., Coster, A.J., Skone, S., Eds.; Elsevier: Amsterdam, The Netherlands, 2020; pp. 121–134. [CrossRef]
125. Tozzi, R.; De Michelis, P.; Coco, I.; Giannattasio, F. A Preliminary Risk Assessment of Geomagnetically Induced Currents over the Italian Territory. *Space Weather* **2019**, *17*, 46–58. [CrossRef]
126. Pezzopane, M.; Pignalberi, A.; Coco, I.; Consolini, G.; De Michelis, P.; Giannattasio, F.; Marcucci, M.F.; Tozzi, R. Occurrence of GPS Loss of Lock Based on a Swarm Half-Solar Cycle Dataset and Its Relation to the Background Ionosphere. *Remote Sens.* **2021**, *13*, 2209. [CrossRef]
127. Marshall, R.A.; Waters, C.L.; Sciffer, M.D. Spectral analysis of pipe-to-soil potentials with variations of the Earth's magnetic field in the Australian region. *Space Weather* **2010**, *8*. [CrossRef]
128. Marshall, R.A.; Smith, E.A.; Francis, M.J.; Waters, C.L.; Sciffer, M.D. A preliminary risk assessment of the Australian region power network to space weather. *Space Weather* **2011**, *9*. [CrossRef]
129. Tozzi, R.; Coco, I.; De Michelis, P.; Giannattasio, F. Latitudinal dependence of geomagnetically induced currents during geomagnetic storms. *Ann. Geophys.* **2019**, *64*, 1–19. [CrossRef]
130. Kahler, S.W. The role of the big flare syndrome in correlations of solar energetic proton fluxes and associated microwave burst parameters. *J. Geophys. Res.* **1982**, *87*, 3439–3448. [CrossRef]
131. Gopalswamy, N.; Yashiro, S.; Liu, Y.; Michalek, G.; Vourlidas, A.; Kaiser, M.L.; Howard, R.A. Coronal mass ejections and other extreme characteristics of the 2003 October-November solar eruptions. *J. Geophys. Res. (Space Phys.)* **2005**, *110*, A09S15. [CrossRef]
132. Wu, C.C.; Liou, K.; Lepping, R.P.; Hutting, L. The 04—10 September 2017 Sun-Earth Connection Events: Solar Flares, Coronal Mass Ejections/Magnetic Clouds, and Geomagnetic Storms. *Sol. Phys.* **2019**, *294*, 110. [CrossRef]
133. Piersanti, M.; De Michelis, P.; Del Moro, D.; Tozzi, R.; Pezzopane, M.; Consolini, G.; Marcucci, M.F.; Laurenza, M.; Di Matteo, S.; Pignalberi, A.; et al. From the Sun to Earth: Effects of the 25 August 2018 geomagnetic storm. *Ann. Geophys.* **2020**, *38*, 703–724. [CrossRef]
134. Xu, S.; Curry, S.M.; Mitchell, D.L.; Luhmann, J.G.; Lillis, R.J.; Dong, C. Magnetic Topology Response to the 2003 Halloween ICME Event at Mars. *J. Geophys. Res. (Space Phys.)* **2019**, *124*, 151–165. [CrossRef]

135. Cramer, A.G.; Withers, P.; Elrod, M.K.; Benna, M.; Mahaffy, P.R. Effects of the 10 September 2017 Solar Flare on the Density and Composition of the Thermosphere of Mars. *J. Geophys. Res. (Space Phys.)* **2020**, *125*, e28518. [CrossRef]
136. Kollhoff, A.; Kouloumvakos, A.; Lario, D.; Dresing, N.; Gómez-Herrero, R.; Rodríguez-García, L.; Malandraki, O.E.; Richardson, I.G.; Posner, A.; Klein, K.L.; et al. The first widespread solar energetic particle event observed by Solar Orbiter on 2020 November 29. *Astron. Astrophys.* **2021**, *656*, A20. [CrossRef]
137. Siciliano, F.; Consolini, G.; Tozzi, R.; Gentili, M.; Giannattasio, F.; De Michelis, P. Forecasting SYM-H Index: A Comparison Between Long Short-Term Memory and Convolutional Neural Networks. *Space Weather* **2021**, *19*, e2020SW002589. [CrossRef]
138. Mumford, S.; Freij, N.; Christe, S.; Ireland, J.; Mayer, F.; Hughitt, V.; Shih, A.; Ryan, D.; Liedtke, S.; Pérez-Suárez, D.; et al. SunPy: A Python package for Solar Physics. *J. Open Source Softw.* **2020**, *5*, 1832. [CrossRef]
139. Price-Whelan, A.M.; Lim, P.L.; Earl, N.; Starkman, N.; Bradley, L.; Shupe, D.L.; Patil, A.A.; Corrales, L.; Brasseur, C.; Nöthe, M.; et al. The Astropy Project: Sustaining and Growing a Community-oriented Open-source Project and the Latest Major Release (v5. 0) of the Core Package. *Astrophys. J.* **2022**, *935*, 167.
140. Forte, R.; Berrilli, F.; Calchetti, D.; Del Moro, D.; Fleck, B.; Giebink, C.; Giebink, W.; Giovannelli, L.; Jefferies, S.M.; Knox, A.; et al. Data reduction pipeline for MOF-based synoptic telescopes. *J. Space Weather Space Clim.* **2020**, *10*, 63. [CrossRef]
141. Giovannelli, L.; Berrilli, F.; Calchetti, D.; Del Moro, D.; Viavattene, G.; Pietropaolo, E.; Iarlori, M.; Rizi, V.; Jefferies, S.M.; Oliviero, M.; et al. The Tor Vergata Synoptic Solar Telescope (TSST): A robotic, compact facility for solar full disk imaging. *J. Space Weather Space Clim.* **2020**, *10*, 58. [CrossRef]
142. Shen, X.; Zong, Q.G.; Zhang, X. Introduction to special section on the China Seismo-Electromagnetic Satellite and initial results. *Earth Planet. Phys.* **2018**, *2*, 439–443. [CrossRef]
143. Mangano, V.; Massetti, S.; Milillo, A.; Plainaki, C.; Orsini, S.; Rispoli, R.; Leblanc, F. THEMIS Na exosphere observations of Mercury and their correlation with in-situ magnetic field measurements by MESSENGER. *Planet. Space Sci.* **2015**, *115*, 102–109. [CrossRef]
144. Leblanc, F.; Doressoundiram, A.; Schneider, N.; Mangano, V.; López Ariste, A.; Lemen, C.; Gelly, B.; Barbieri, C.; Cremonese, G. High latitude peaks in Mercury's sodium exosphere: Spectral signature using THEMIS solar telescope. *Geophys. Res. Lett.* **2008**, *35*, L18204. [CrossRef]
145. Piersanti, M.; Villante, U. On the discrimination between magnetospheric and ionospheric contributions on the ground manifestation of sudden impulses. *J. Geophys. Res. (Space Phys.)* **2016**, *121*, 6674–6691. [CrossRef]
146. Mura, A.; Milillo, A.; Orsini, S.; Massetti, S. Numerical and analytical model of Mercury's exosphere: Dependence on surface and external conditions. *Planet. Space Sci.* **2007**, *55*, 1569–1583. [CrossRef]